

## Acoustical force nanolithography of thin polymer films

F. J. Rubio-Sierra<sup>1</sup>, A. Yurtsever<sup>1</sup>, M. Hennemeyer<sup>1</sup>, W. M. Heckl<sup>1,2</sup>, and R. W. Stark<sup>\*,1</sup>

<sup>1</sup> CeNS and Crystallography, Department of Earth and Environmental Sciences, Ludwig-Maximilians-Universität München, Theresienstr. 41, 80333 München, Germany

<sup>2</sup> Deutsches Museum, Museumsinsel 1, 80538 München, Germany

Received 30 September 2005, revised 16 December 2005, accepted 17 December 2005

Published online 4 April 2006

PACS 07.79.Lh, 68.37.Ps, 81.16.Nd

Nanomachining of thin polymer resist films with an atomic force microscope (AFM) is a promising route for the fabrication of nanoscale devices. In order to enhance the controllability of the nanomachining process an in-plane acoustic wave is coupled to the sample support. This enhances the intermittent force exerted by the AFM tip. The lateral resolution reached by this method is only limited by the physical size of the AFM tip to dimensions far below the light diffraction limit. The main process parameters are the frequency and magnitude of the acoustic wave, and the preloading force. In this work, the feasibility of acoustical force lithography and the influence of the relevant parameters are investigated.

© 2006 WILEY-VCH Verlag GmbH & Co. KGaA, Weinheim

### 1 Introduction

Surface patterning at the smallest scale is a key issue for the further development of technological and scientific applications that require rapid prototyping of nanostructures. Currently, optical lithography is the standard technique for the fabrication of structured surfaces. However, the lateral resolution of optical lithography is limited by diffraction. To overcome this limitation, alternative surface patterning methods have been developed during the last years, such as e-beam lithography, masked deposition, scanning probe techniques, or microcontact printing [1]. Scanning probe microscope related techniques represent the most versatile approach for rapid prototyping of lateral nanoscale structures [2, 3]. Among the members of the scanning probe family, the atomic force microscope (AFM) has experienced an impressive development for its application to lithography [4, 5]. Essentially, there are three physically different types of AFM lithography: local anodic oxidation [6], surface chemical patterning [7], and mechanical machining [8]. Mechanical machining by AFM has the main advantages of being a direct method – it is not restricted to functional materials. The resolution is only limited by the physical dimensions of the AFM tip, which is much smaller than the light diffraction limit.

Currently, two different approaches are used for mechanical machining by AFM. The quasi-static approach relies on the application of a static load on the sample to produce plastic deformation while the AFM tip moves on the surface [9]. The main drawback of the quasi-static method is the poor controllability of the process due to lateral forces [10]. In the second approach, dynamic mechanical machining, the AFM cantilever is oscillated with a small amplitude which minimizes unwanted lateral forces during the lithography process. Typically, the supporting piezo-element is used to generate cantilever oscillations by the excitation of flexural resonant modes. If the AFM tip is sufficiently close to the sample and the excitation is strong enough, nanostructures can be lithographed on the surface. This method is also found in the literature as dynamic plowing lithography [11].

\* Corresponding author: e-mail: stark@nanomanipulation.de, Phone: +49 89 2180 4329, Fax: +49 89 2180 4334

The controllability of standard dynamic plowing is limited by the fact that the cantilever actuation depends strongly on the transfer characteristics of the dithering piezo-element and the cantilever: The fixed end actuation of the cantilever introduces a time-delay in the system between the actuation and the tip. This can limit the bandwidth of high-speed closed-loop control of the machining process [12]. Additionally, the non-linear tip-sample interaction produces a strong shift of the cantilever resonant frequency. Thus, a promising method for cantilever excitation is to couple a normal incidence shear acoustic wave to the cantilever tip through sample surface. The acoustic wave is generated by an acoustic transducer below the sample [13, 14].

In the following, we discuss ‘acoustical force nanolithography’, a surface machining method based on the AFM. In order to avoid the hardly controllable stick-slip oscillations of quasi-static plowing lithography, the oscillations are induced by a normal incidence shear acoustic wave. Prior to lithography, the frequency response of the cantilever is acquired to obtain the optimal frequency of operation. The influence of the main experimental parameters such as excitation frequency, amplitude, and the preloading force is investigated in detail.

## 2 Experimental and methods

The experiments were carried out on a Dimension 3100 Scanning Probe Microscope System (Veeco Metrology, Santa Barbara, CA). Lithography paths were programmed using the NanoMan II software of the instrument. For the process parameters characterization, a triangular cantilever with a nominal force constant of 48 N/m was used (NSC11, MikroMasch, Tallinn, Estonia). For the lithography a rectangular cantilever with a nominal force constant of 40 N/m was used (NSC16, MikroMasch, Tallinn, Estonia). As illustrated in Fig. 1, the sample was mounted on a normal incidence shear wave transducer (v153, Panametrics-NDT, Waltham, MA). For lithography a continuous sinusoidal signal was coupled to the ultrasonic transducer. To switch between imaging and lithography mode, the sample bias voltage signal of the AFM controller was used as trigger signal; this signal can be accessed through a signal access module. In this modified lithography system the sample holder is electrically isolated from the sample bias voltage signal of the controller.

Samples were prepared on silicon chips with a size of about 1 cm<sup>2</sup>. Prior to coating, the chips were cleaned with acetone, isopropanol, and de-ionized water. A thin polymer film was prepared by spin coating ( $\omega = 500 \text{ min}^{-1}$  for 30 s,  $\omega = 5000 \text{ min}^{-1}$  for 60 s) *ma-p 1205*<sup>®</sup> (based on Novolak, naphthoquinone diazide, and solvents; MicroChem, Newton, MA). After spinning, the samples were dried on a hot plate at 100 °C for 40 s.

All images were acquired in standard tapping mode where the dither piezo of the cantilever holder is used for excitation. For image processing a commercial software package was used (SPIP 4.0, Image Metrology A/S, Lyngby, Denmark). In order to obtain a reliable measurement of the width of the litho-

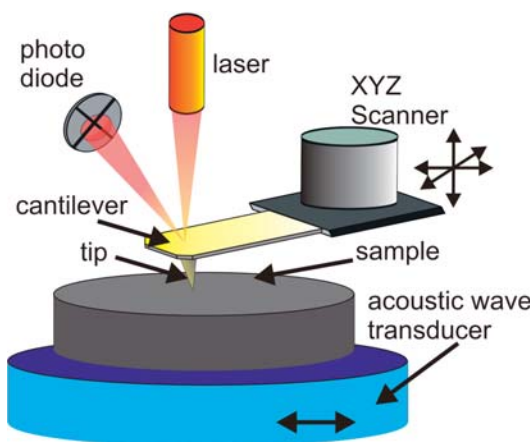


**Fig. 1** (online colour at: [www.pss-a.com](http://www.pss-a.com)) Schema of the experimental setup for acoustical force nanolithography. The sample holder consists on an acoustic wave transducer that is used to enhance cantilever flexural vibrations for lithography.

graphed structures, the influence of the tip-shape on the measured topography had to be considered. Due to the geometric ‘convolution’ of the tip shape with the surface profile the width of grooves is underestimated in the raw topographic data. Thus, the images were low-pass filtered to remove high frequency noise. Then, a worst-case tip shape was estimated employing the tip characterization procedure of the software package [15]. In order to obtain reliable upper limits for the width of the nanomachined lines, the tip shape was deconvoluted from topographic data [16].

### 3 Process parameters

#### 3.1 Resonance spectra

In order to tune the excitation frequency for lithography the frequency response of the cantilever to a continuous single tone excitation of the ultrasonic transducer was analyzed. Two different types of vibration spectra were acquired: one for the free cantilever and one for the surface-coupled cantilever. The excitation frequency was swept stepwise in the frequency band from 400 kHz to 1 MHz. The vibration spectra of the AFM cantilever were measured by demodulation of the deflection signal with an external lock-in amplifier (7280, Ametek, Oak Ridge, TN). The frequency response of the free cantilever is shown in Fig. 2(a). The cantilever was placed about 2  $\mu\text{m}$  over the sample surface during the measurement of the frequency response. The out-of plane oscillations of the vibrations of the ultrasonic transducer couple through the air to the cantilever. Only one resonant peak appears at a frequency of 423.4 kHz within the analyzed frequency band.

In order to acquire the resonance spectra of the surface-coupled cantilever, the vibrating AFM cantilever is brought into intermittent contact by approaching the cantilever to the surface until the AFM cantilever oscillation amplitude was reduced to 20%. Then, the microscope feedback-loop was disconnected and the vibration spectrum was acquired. Figure 2(b) shows the vibration spectrum with several resonant peaks. The main resonance peak is shifted and obscured by new resonances in the spectrum. These new resonances are caused by the strong non-linear character of the tip-sample interaction and resonances in the frequency response of the acoustic transducer [17, 18]. Six major resonant peaks are located at  $f = 477.0, 598.2, 637.8, 777.2, 879.6,$  and  $940.8$  kHz. The response of the system close to 1 MHz is enhanced due to the frequency response of the acoustic wave transducer which is centered at this frequency.

#### 3.2 Acoustic wave frequency

The frequency response of the surface-coupled cantilever shows that the vibration amplitude depends strongly on the excitation frequency. Four traces were lithographed at different resonant peaks of the surface-coupled cantilever frequency response in order to characterize the influence of the excitation frequency (1 Volt signal amplitude). Figure 3(a) shows the resulting traces and the height profile. All lines successfully ploughed grooves on the sample surface. Residual material from the plowing process

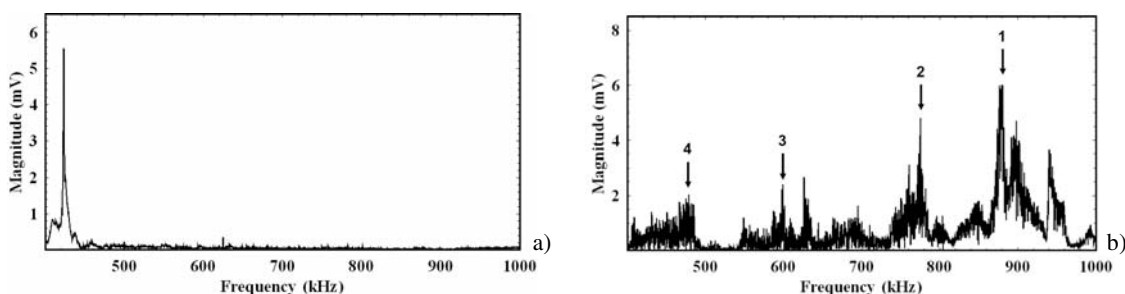


**Fig. 2** Vibration spectra of: a) the freely vibrating cantilever, and b) the surface-coupled cantilever. The numbered peaks in (b) were used to characterize the influence of the frequency response in the lithography process.

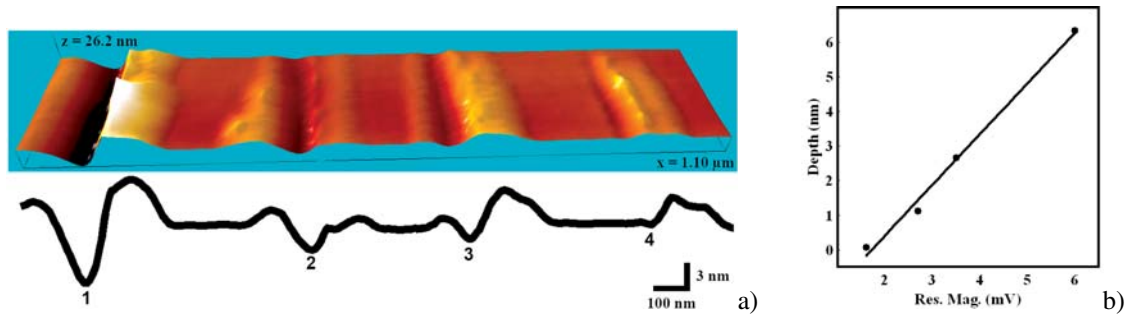


**Fig. 3** (online colour at: [www.pss-a.com](http://www.pss-a.com)) Variation of lithography depth with the resonant magnitude of the surface-coupled frequency response (Fig. 2). The resonant magnitudes and corresponding excitation frequencies for the four different traces were: trace 1, 6.0 mV (at 879.4 kHz); trace 2, 3.5 mV (at 774.2 kHz); trace 3, 2.7 mV (at 626 kHz); trace 4, 1.6 mV (at 479.4 kHz). a) 3D-representation and height profile of the patterned area. b) Increase of lithographed depth with the frequency response magnitude of the resonant peak. A linear fit of the experimental data is also displayed.

appears at both sides of the grooves. From the results it is clearly seen that the lithographed depth is directly related to which resonant peak is used to generate the acoustic wave. Figure 3(b) shows that the lithographed trace depth increases linearly with the magnitude of the resonant peak.

### 3.3 Acoustic wave amplitude

The vibration amplitude of the surface-coupled cantilever and, consequently, the applied tip-sample forces, directly depends on the magnitude of the excitation. To characterize the influence of the acoustic wave amplitude on the lithography process, six lines were lithographed using the same frequency (940.8 kHz) but at different magnitudes of the excitation signal.

The first trace was performed without acoustic wave excitation. All the lines traced with acoustic wave excitation resulted in the fabrication of grooves. Figure 4(b) shows a slight deviation from a linear relation between acoustic wave magnitude and lithographed depth. From Fig. 4(a) it is evident that the sample surface appears raised next to the groove. Raised polymer areas after quasi-static machining for loads below the yield strength of the polymer have been previously reported [9]. However, the mechanism for this material displacement is not well understood. Morphological changes induced by viscoelastic effects or localized heat have been proposed as origins of this phenomenon.

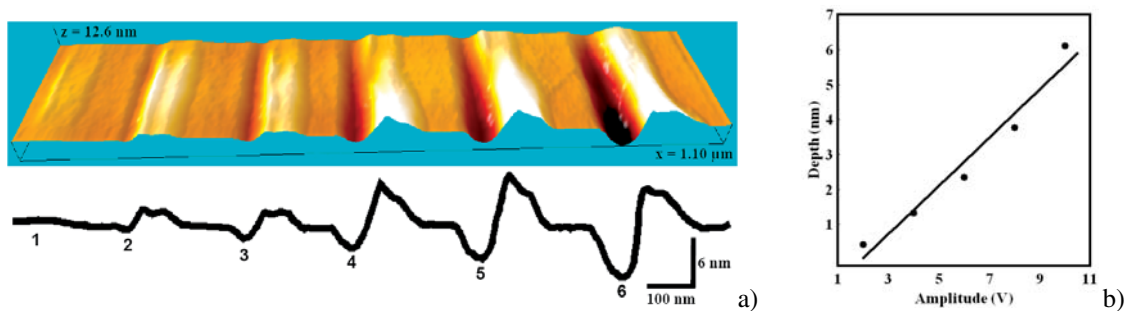


**Fig. 4** (online colour at: [www.pss-a.com](http://www.pss-a.com)) Increase in lithography depth with the magnitude of the excitation signal. The signal amplitudes for the five different traces were: trace #1, 0 V; trace #2, 2 V; trace #3, 4 V; trace #4, 6 V; trace #5, 8 V; trace #6, 10 V. a) 3D-representation and height profile of the patterned area. b) Relation between lithographed depth and signal magnitude. A linear fit of the experimental data is also displayed.

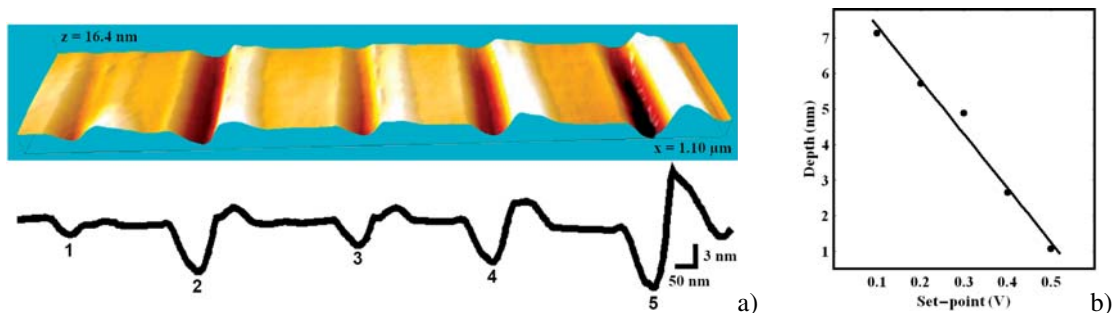


**Fig. 5** (online colour at: [www.pss-a.com](http://www.pss-a.com)) Variation of lithography depth with set-point of the topography feedback. The corresponding set-points were: trace 1, 0.5 V; trace 2, 0.2 V; trace 3, 0.4 V; trace 4, 0.3 V; trace 5, 0.1 V. a) 3D-representation and height profile of the patterned area. b) Decrease of lithographed depth with increasing set-point. A linear fit of the experimental data is also displayed.

### 3.4 Preloading force

The coupling of the acoustic wave to the AFM tip depends on the cantilever preloading force. The preloading force is determined by the set-point of the topography feedback prior to lithography. A lower set-point corresponds to a greater preloading force.

Thus, a dependency between the lithographed depth and the preloading force can be expected. To illustrate this, five lines were lithographed at different set-points while applying an excitation signal of 1 V of amplitude at the main resonant peak of the surface-coupled cantilever frequency response (at 879.4 kHz). As expected, a decrease of lithographed depth with increasing set-point is observed in Fig. 5. This dependence has a linear character within the investigated range as seen in Fig. 5(b).

Figure 6 shows two lithographed structures demonstrating the feasibility of the method for the generation of nanostructures. Figure 6(a) shows the lithographed emblem of the Ludwig Maximilians University.

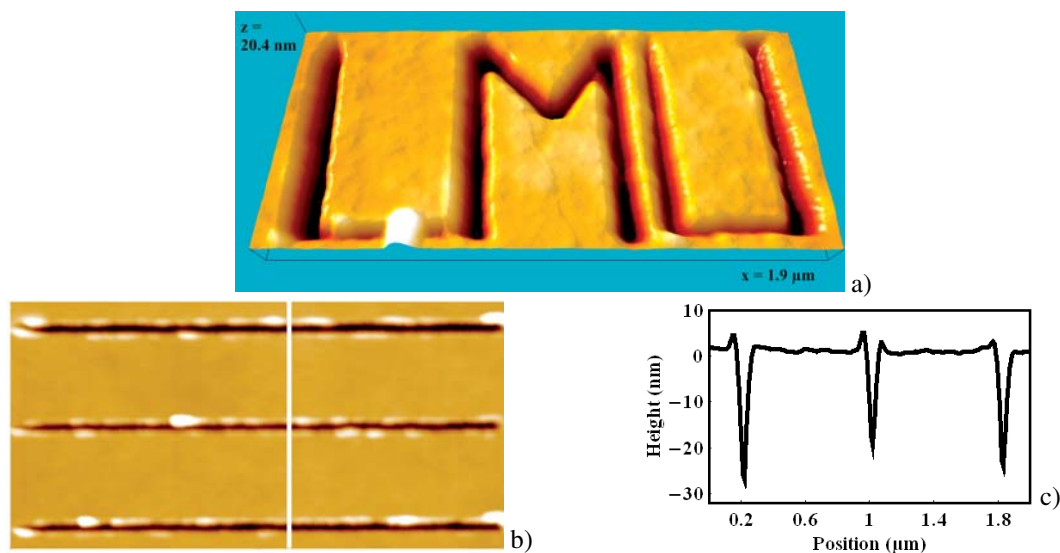


**Fig. 6** (online colour at: [www.pss-a.com](http://www.pss-a.com)) Nanostructures generated by acoustical force nanolithography: a) lithographed emblem of the Ludwig-Maximilians-University. b) AFM image of three 4  $\mu\text{m}$  long lines lithographed using a signal amplitude of 0.5 V at a frequency of 740 kHz for acoustic wave generation, with an average tip-sample distance of 12.7 nm. Image size (4  $\times$  2  $\mu\text{m}$ ) and z-range of 55.6 nm. c) Line profile along the white line in panel b.

Figure 6(b) and (c) show the AFM image and height profile of three lithographed lines with a length of 4  $\mu\text{m}$ . The average line width at FWHM was of 50 nm. The parameters were chosen to reach a line depth greater than 20 nm. This is relevant for the application of this method as first step in high resolution lift-off lithography, where thin resist layers with a thickness about 20 nm are used [19].

## 4 Conclusions

Acoustical force nanolithography is an AFM lithography method providing control on the machining process by actuation of AFM cantilever through the specimen by an acoustic wave. A precise control can be achieved by tuning the excitation frequency and amplitude of the excitation to purpose. The feasibility of the method along with the characterization of the main parameters was illustrated by lithography of a thin resist film. After initial tuning of the machining forces by fine tuning the excitation frequency, amplitude and set point, the nanolithography process is a reliable process.

Due to the reduced physical dimensions of the AFM tip and precise positioning and force control provided by acoustic force nanolithography, lateral dimensions of the lithographed traces are reduced far beyond light diffraction limit. The method is easy to implement in probe-scanning AFM configurations and can be used as a stand-alone method for surface modification or as complement for fine adjustment of standard mechanical machining of surfaces by AFM.

**Acknowledgements** Funding by the German Federal Ministry of Education and Research (BMBF) under grant 03N8706 is gratefully acknowledged. F. J. Rubio-Sierra thanks the Elite Network of Bavaria for financial support.

## References

- [1] M. Geissler and Y. Xia, *Adv. Mater.* **16**, 1249 (2004).
- [2] A. A. Tseng, A. Notagiacomo, and T. P. Chen, *J. Vac. Sci. Technol. B* **23**, 877 (2005).
- [3] D. Wouters and U. S. Schubert, *Angew. Chem. Int. Ed.* **43**, 2480 (2004).
- [4] F. J. Rubio-Sierra, W. M. Heckl, and R. W. Stark, *Adv. Eng. Mater.* **7**, 193 (2005).
- [5] D. Fotiadis, S. Scheuring, S. A. Müller, A. Engel, and D. J. Müller, *Micron* **33**, 385 (2002).
- [6] R. Garcia, M. Calleja, and H. Rohrer, *J. Appl. Phys.* **86**, 1898 (1999).
- [7] S. Krämer, R. R. Fuierer, and C. B. Gorman, *Chem. Rev.* **103**, 4367 (2003).
- [8] T. A. Jung, A. Moser, H. J. Hug, D. Brodbeck, R. Hofer, H. R. Hidber, and U. D. Schwarz, *Ultramicroscopy* **42**, 1446 (1992).
- [9] X. Jin and W. N. Unertl, *Appl. Phys. Lett.* **61**, 657 (1992).
- [10] R. W. Stark, S. Thalhammer, J. Wienberg, and W. M. Heckl, *Appl. Phys. A* **66**, S579 (1998).
- [11] M. Heyde, K. Rademann, B. Cappella, M. Geuss, H. Sturm, T. Spangenberg, H. Niehus, *Rev. Sci. Instrum.* **72**, 136 (2001).
- [12] F. J. Rubio-Sierra, R. Vázquez, and R. W. Stark, in: *Proceedings of IMECE2005 2005, ASME International Mechanical Engineering Congress and Exposition, November 5–11, 2005, Orlando, Florida, USA.*
- [13] A. Caron, U. Rabe, M. Reinstädler, J. A. Turner, and W. Arnold, *Appl. Phys. Lett.* **85**, 6398 (2004).
- [14] C. K. Hyon, S. C. Choi, S. W. Hwang, D. Ahn, Y. Kim, and E. K. Kim, *Jpn. J. Appl. Phys.* **38**, 7257 (1999).
- [15] J. S. Villarrubia, *J. Natl. Inst. Stand. Technol.* **102**, 435 (1997).
- [16] R. W. Stark, F. J. Rubio-Sierra, S. Thalhammer, and W. M. Heckl, *Eur. Biophys. J.* **32**, 33 (2003).
- [17] U. Rabe, K. Janser, and W. Arnold, *Rev. Sci. Instrum.* **67**, 3281 (1996).
- [18] R. W. Stark, G. Schitter, M. Stark, R. Guckenberger, and A. Stemmer, *Phys. Rev. B* **69**, 085412 (2004).
- [19] C. Martin, G. Rius, X. Borrísé, and F. Pérez-Murano, *Nanotechnology* **16**, 1016 (2005).